

Initial Pb isotopic compositions of lunar granites as determined by ion microprobe

W. COMPSTON,¹ I. S. WILLIAMS¹ and C. MEYER²

¹Research School of Earth Sciences, The Australian National University, Canberra, Australia

²NASA, Johnson Space Center, Houston, TX, U.S.A.

Abstract—The Pb isotopic compositions of selected areas within lunar feldspars were measured *in situ* on the SHRIMP ion microprobe at sensitivity up to 140 cps/ppm Pb. Usable data were obtained at the 1 ppm level, with analytical Pb blank ≤ 0.2 femtograms. The highest Pb content, 30 ppm, was found in Ba-rich feldspar in a felsite fragment from breccia 14163. There was no detectable U or Th and the Pb isotopic composition was uniform and highly radiogenic: very high $^{207}\text{Pb}/^{206}\text{Pb}$ at 1.50 ± 0.02 (2σ) with very low $^{204}\text{Pb}/^{206}\text{Pb}$ at 0.0029 ± 0.0002 . It represents the true initial Pb ratios of the felsite magma, which must have been generated from a long-lived source having very high $^{238}\text{U}/^{204}\text{Pb}$ (μ) ≈ 1500 . Multiple analyses of plagioclase and K-feldspar from a ≥ 4.32 Ga granite clast 14303, 1027 show high $^{207}\text{Pb}/^{206}\text{Pb}$ averaging 1.56, but with a distinct internal $^{207}\text{Pb}/^{206}\text{Pb}$ vs. $^{208}\text{Pb}/^{206}\text{Pb}$ trend. The latter suggests addition of radiogenic Pb formed in U-rich minerals outside the analysed areas, presumably as a result of thermally induced Pb isotope exchange during a metamorphism at 3.5–4.0 Ga. Consequently, the true initial $^{207}\text{Pb}/^{206}\text{Pb}$ for the granite would be at least 1.65, with an upper limit of 1.78, corresponding to single-stage U-Pb evolution from 4.55 Ga to 4.32 Ga in a high- μ (*ca.* 1500) source.

K-feldspars from a clast of VHK basalt from breccia 14305 also contain highly radiogenic Pb and have a single-stage model age of 3.81 ± 0.07 Ga, within error of the Rb-Sr crystallization age of 3.75 Ga. The radiogenic initial Pb requires high μ at 1120 for a single-stage source, or greater for a variety of two-stage source models. If the Pb is truly indigenous, and not hybridized by assimilation of lunar granite, then the VHK basalt source must have high μ , in contrast to other mare basalts which have comparatively low μ . Plagioclase from the quartz monzodiorite clast in 15405 records radiogenic initial Pb but extremely low contents of U and Th, which contrasts with thermal ionization results for mineral grains from the same rock.

High $^{207}\text{Pb}/^{206}\text{Pb}$ Pb values in many feldspar-rich fragments have been attributed to internal equilibration between U-rich and Pb-rich minerals that formed originally at 4.42 Ga, during a late lunar cataclysm at *ca.* 3.9 Ga. Radiogenic initial Pb at 4.4 Ga is not allowed in this model. Our data imply, on the contrary, that there must be some lunar initial Pb with $^{207}\text{Pb}/^{206}\text{Pb} > 1.65$ that evolved earlier than 4.3 Ga in an extremely high μ environment. No metamorphism is needed for the 3.9 Ga granites, and a younger metamorphism would suffice for one of the 4.3 Ga granites. The implication for lunar history is that there was very early Pb loss from large volumes of the Moon, and later igneous production of lunar granite labelled by high $^{207}\text{Pb}/^{206}\text{Pb}$ from this long-lived Pb-depleted material.

INTRODUCTION

THE INITIAL Pb isotopic compositions of lunar highland rocks remain poorly defined, making it difficult to trace the early evolution of lunar $^{238}\text{U}/^{204}\text{Pb}$ (“ μ ”). It is known that at some time close to 4.5 Ga, much or all of the assembled Moon lost Pb relative to U, thereby acquiring a high μ relative to the Earth (SILVER, 1970; TATSUMOTO, 1970). In addition, Pb loss from the Moon was evidently not uniform; the deep source rocks for mare basalts have comparatively low μ (~ 30 , TATSUMOTO *et al.*, 1987) whereas some of the anorthositic remnants of the oldest lunar crust have high measured μ (TERA *et al.*, 1984).

Direct measurement of lunar initial Pb is especially difficult because of the very low Pb contents of lunar highland rocks, and, in addition, interpretation is complicated by their complex thermal histories due to meteoritic bombardment. Highly ra-

diogenic Pb was present in feldspars at ~ 3.9 Ga (TERA *et al.*, 1974). Was it wholly metamorphic in origin due to isotopic resetting during a “terminal cataclysm,” or was there radiogenic initial Pb at, say, 4.4 Ga generated in still older high- μ rocks?

We applied the ion probe to this question primarily in the course of U-Pb age determinations on lunar zircons. In principle, the precision for U-Pb ages by ion probe for old zircons can be as high as a few million years, but this cannot be realized without reliable knowledge of the initial Pb isotopic composition. There were internal indications of a high- μ initial Pb at 4.35 Ga from our first lunar zircon measurements (COMPSTON *et al.*, 1984), but the particular zircons, being rounded grains in breccia, were not relatable texturally to adjacent minerals that might have enough initial Pb to measure. The later discovery, in several lunar granites, of euhedral zircons associated with Pb-rich K-feld-

spars (MEYER *et al.*, 1985) provided the necessary cogenetic link. Such feldspars should contain original magmatic Pb appropriate to the adjacent zircons, and, moreover, their age will be accurately and independently known through the zircon dating itself. The combination of magmatic Pb compositions and known ages is exactly what is necessary to explore and possibly define growth-curves for lunar Pb, making *in situ* Pb isotope analyses of dated feldspars an important isotopic database.

METHODS

Our first priority for feldspar Pb analysis was maximum sensitivity, to have enough Pb counts N per mass during an analysis period of *ca.* 20 minutes to obtain usable statistical precision ($1/\sqrt{N}$). At the same time, we elected to operate at the usual zircon mass-resolution of 5500 (2% definition) to reduce the possibility of low level isobaric interferences that might become appreciable at sub-ppm Pb and U levels. Sensitivity was enhanced first by matching the large acceptance of the SHRIMP mass-analyser (CLEMENT and COMPSTON, 1989) with the largest probe size allowed by the fractured nature of the feldspar crystals, a $25 \times 35 \mu\text{m}$ ellipse (Fig. 1) and secondly by use of the highest sputtering rate available for this probe size, *ca.* 20 $\mu\text{m}/\text{h}$ for 12 nA of total negative oxygen in the primary beam. Under these conditions, the sensitivity was *ca.* 10 cps/ppm Pb/nA based on the count-rate obtained for a K-feldspar standard of known Pb content that was mounted with the lunar polished thin-sections. The precision of the measured isotope ratios is controlled almost entirely by the total number of ions counted during the analysis, which depends in turn on the Pb contents of the particular target. For $^{207}\text{Pb}/^{206}\text{Pb}$, it ranged from a best of 0.6% (σ) in feldspar having the greatest Pb content, to as poor as 10% for a few areas below 0.1 ppm. For many feldspars it was around 3% which, although high, is nevertheless adequate to address the problem because of the Moon's uniquely high average μ .

Data collection was similar to that described for zircon U-Pb dating (COMPSTON *et al.*, 1984). The mass stations in the peak switching cycle were confirmed using a reference zircon and Pb-rich feldspar. U and Th in the feldspars were monitored at UO^+ and ThO^+ , automatic peak-centering was used for ^{206}Pb only, and ^{204}Pb was counted for 40 seconds per scan because of its extreme depletion on the Moon. Each analysis took about 17 minutes for seven scans.

Between our first analyses of lunar feldspars (COMPSTON *et al.*, 1989) and the present, the SHRIMP primary column was modified to operate in Köhler illumination mode (LIEBL, 1984). This changed the ion-density profile of the probe from "Gaussian," which produced at best a conical pit often with a wide diffuse ion halo, to a very even profile giving a flat-bottomed pit with sharply defined edges and no halo (Fig. 1). The important consequence is rapid removal of surface-related Pb; the polished but contaminated sample surface is quickly and uniformly removed by sputtering before the start of data collection. We are confident that (almost) all common Pb remaining is located within the body of the target and therefore properly belongs to the analysis. In addition, the probe initially is rastered automatically about the selected area which cleans the surface immediately outside the (future) pit-edges.

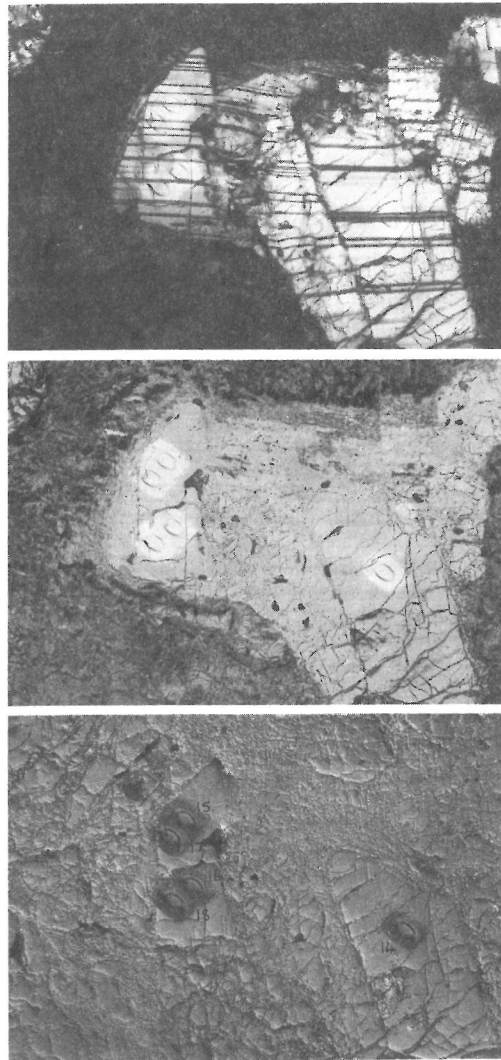


FIG. 1. Photomicrographs of thin section 14303, 205 showing a closely fractured plagioclase crystal in crossed polarised, plane polarised, and reflected light, respectively. Pits left after ion probe analysis of the least fractured regions are clearly visible. Each pit is surrounded by a rectangular etch mark produced by raster pre-cleaning of the sample's surface. Field of view *ca.* $550 \times 750 \mu\text{m}$.

A "processing blank" for the analysis method can be estimated from the results for plagioclase in 14305, 393, which has an apparent Pb content of *ca.* 0.025 ppm (Table 1). In striking contrast to the associated K-feldspar, its measured $^{207}\text{Pb}/^{206}\text{Pb}$ and $^{208}\text{Pb}/^{206}\text{Pb}$ are equal to modern terrestrial Pb, indicating that all of the plagioclase Pb is probably contamination (Fig. 11). (This is not so for $^{204}\text{Pb}/^{206}\text{Pb}$, but the latter should be disregarded as only two ^{204}Pb ions were detected during the whole analysis.) The amount of Pb determined in the plagioclase can be estimated at 2×10^{-16} g from its apparent Pb concentration and the weight of feldspar consumed during analysis (*ca.* 8 ng). This extremely small amount, equivalent to about

half a million Pb atoms, is the blank. Its origin might be terrestrial Pb atoms on the surface of the polished section that are "knocked on" during sputtering, or residual surface Pb that continues to be slowly sputtered from the pit edges. In either case, the blank would be reduced by chemical cleaning of the surface prior to ion probe analysis.

For the present work, we expect that the blank varied according to the contamination of individual sample surfaces. For example, the measured $^{208}\text{Pb}/^{206}\text{Pb}$ for the low-Pb area 33.2 in granite 14303 (Table 1) indicates that ca. 90% of the measured Pb is initial feldspar Pb and therefore that the analytical blank is $\times 10$ lower than for 14305, 393. We also expect to see variation in Pb isotope ratios caused by the irregular presence of injected meteoritic material, which is known to occur in all but the most "pristine" lunar samples.

PB ISOTOPE MODELLING

Measurements of ^{204}Pb by ion probe are imprecise compared with thermal ionisation owing to the much smaller amount of Pb used for the analysis (typically $\times 10^{-3}$). Consequently, we have not employed the traditional $^{207}\text{Pb}/^{204}\text{Pb}$ vs. $^{206}\text{Pb}/^{204}\text{Pb}$ diagram for modelling Pb isotope evolution in order to avoid the strong y, x correlation generated in this plot by errors in ^{204}Pb . Instead, we use $^{207}\text{Pb}/^{206}\text{Pb}$ vs. $^{204}\text{Pb}/^{206}\text{Pb}$ and $^{207}\text{Pb}/^{206}\text{Pb}$ vs. $^{208}\text{Pb}/^{206}\text{Pb}$.

Secondary isochrons

For the above diagrams the starting point for Pb isotope modelling, the Canyon Diablo troilite, plots on the right-hand side (Fig. 2a,b). (Regardless of the exact age of the Moon, its starting Pb or that of its antecedents before assembly would derive ultimately from this primordial source.) Purely radiogenic Pb accumulated between times T_0 and T_1 (single-stage evolution with infinite μ) is located on the $^{207}\text{Pb}/^{206}\text{Pb}$ axis in Fig. 2a at zero $^{204}\text{Pb}/^{206}\text{Pb}$. Its value is determined solely by T_0 and T_1 :

$$\frac{^{207}\text{Pb}_*/^{206}\text{Pb}_*}{=} = (e^{\lambda_5 T_0} - e^{\lambda_5 T_1}) / (e^{\lambda_8 T_0} + e^{\lambda_8 T_1}) / R \quad (1)$$

where * denotes radiogenic Pb, λ_5, λ_8 the $^{238}\text{U}, ^{235}\text{U}$ decay constants, and R the present-day $^{238}\text{U}/^{235}\text{U}$. It constitutes the slope for secondary isochrons on the traditional plot.

In Fig. 2b, the x -value for purely radiogenic Pb will be

$$\frac{^{208}\text{Pb}_*/^{206}\text{Pb}_*}{=} = (^{232}\text{Th}/^{238}\text{U})(e^{\lambda_2 T_0} + e^{\lambda_2 T_1}) / (e^{\lambda_8 T_0} + e^{\lambda_8 T_1}) \quad (2)$$

so that a value for present-day $^{232}\text{Th}/^{238}\text{U}$ must be assumed.

In Fig. 2a, secondary isochrons are the straight lines joining the T_1 radiogenic end-member on the

$^{207}\text{Pb}/^{206}\text{Pb}$ axis with the Canyon Diablo point. In Fig. 2b, they join the T_1 radiogenic $^{207}\text{Pb}_*/^{206}\text{Pb}_*$, $^{208}\text{Pb}_*/^{206}\text{Pb}_*$ point with Canyon Diablo. When T_1 is the known age of the feldspar, its Pb isotope ratios must lie on the T_0 to T_1 secondary isochron for single-stage evolution. If it does not, two-stage evolution of the magma source is possible but only within defined limits (see below). If it falls beyond the two-stage limits, a post-magmatic metamorphic change in isotopic composition must be inferred.

Reference isochrons for 3.9 Ga and 4.35 Ga, appropriate for the lunar granites, are drawn on Fig. 2a and b.

Growth curves

Pb isotope ratios at times T_1 , evolved in single-stages of constant μ from common Pb at T_0 having isotope ratios relative to ^{204}Pb of X_0, Y_0, Z_0 , are given by

$$(^{206}\text{Pb}/^{204}\text{Pb})_1 = X_1 = X_0 + \mu(e^{\lambda_8 T_0} + e^{\lambda_8 T_1}) \quad (3)$$

$$(^{207}\text{Pb}/^{204}\text{Pb})_1 = Y_1 = Y_0 + \mu/R(e^{\lambda_5 T_0} + e^{\lambda_5 T_1}) \quad (4)$$

$$(^{208}\text{Pb}/^{204}\text{Pb})_1 = Z_1 = Z_0 + \mu(^{232}\text{Th}/^{238}\text{U}) \times (e^{\lambda_2 T_0} + e^{\lambda_2 T_1}) \quad (5)$$

which are transformed to the Fig. 2 coordinates as

$$(^{204}\text{Pb}/^{206}\text{Pb})_1 = 1/X_1$$

$$(^{207}\text{Pb}/^{206}\text{Pb})_1 = Y_1/X_1$$

$$(^{208}\text{Pb}/^{206}\text{Pb})_1 = Z_1/X_1.$$

Single-stage growth curves from Canyon Diablo Pb have been plotted in Fig. 2 at various μ values from a low of 9.0 as for terrestrial Pb, to a high of 2000, which approximates the lunar granites.

Two-stage Pb evolution

A more complex history of the magma source (and/or the metamorphic history of the feldspar) must be considered if the feldspar isotopic ratios do not lie on a single-stage isochron equivalent to its known age. Equation (3) above may be generalised to represent Pb isotope evolution in two successive U/Pb regimes for the magma source, specified as μ_0 and μ_1 for the time-periods T_0 to T_1 and T_1 to T_2 :

$$(^{206}\text{Pb}/^{204}\text{Pb})_2 = X_0 + \mu_0(e^{\lambda_8 T_0} + e^{\lambda_8 T_1}) + \mu_1(e^{\lambda_8 T_1} - e^{\lambda_8 T_2}). \quad (6)$$

The term $(^{206}\text{Pb}/^{204}\text{Pb})_2$ is the initial ratio in the feldspar on crystallisation at T_2 , when the production of the granite magma terminated the μ_1 regime.

Table 1. U-Th-Pb analyses of lunar feldspars using the SHRIMP ion microprobe; "cts" refers to total ions counted during the analysis.

Sample	204/206	±	207/206	±	208/206	±	206 cts	UO cts	ThO cts	Pb ppm	U ppb	Th ppb
12033, 567												
K3	0.001	0.000	1.329	0.015	0.878	0.006	12826	16	56	4.2	5.0	17.5
K4	0.001	0.000	1.304	0.015	0.841	0.005	13524	0	0	4.3	0.0	0.0
K5	0.001	0.000	1.297	0.016	0.895	0.015	12107	208	877	3.8	68.7	289.8
K6	0.002	0.000	1.174	0.014	0.897	0.017	12912	0	1	3.9	0.0	0.3
PL3	0.002	0.001	1.194	0.036	0.938	0.024	2000	0	75	0.6	10.0	150.0
PL4	0.005	0.001	1.174	0.038	0.921	0.033	1706	19	59	0.5	44.5	138.3
PL5	0.004	0.001	1.219	0.037	1.012	0.044	1892	107	265	0.6	226.2	560.3
K1, 1988	0.003	0.002	1.306	0.025	0.933	0.012	2072	10	26			
K2, 1988	0.000	0.000	1.238	0.013	0.959	0.017	2192	1	14			
K3, 1988	0.000	0.000	1.319	0.021	0.846	0.010	14398	1	3			
K4, 1988	0.000	0.000	1.355	0.009	0.864	0.011	16531	0	0			
14321, 1047												
K4	0.001	0.000	1.471	0.019	0.771	0.015	10176	0	13	3.2	0.0	5.1
K5	0.001	0.000	1.422	0.011	0.734	0.005	29080	2	3	9.1	0.3	0.4
K6	0.001	0.000	1.415	0.011	0.720	0.006	30077	1	3	9.3	0.1	0.4
K7	0.001	0.000	1.432	0.011	0.724	0.005	29410	0	10	9.2	0.0	1.4
K8	0.001	0.000	1.463	0.011	0.727	0.005	27247	6	5	8.7	0.9	0.7
K9	0.001	0.000	1.414	0.012	0.731	0.006	24569	0	5	7.8	0.0	0.8
K1, 1988	0.002	0.000	1.398	0.009	0.759	0.005	41077	0	0			
K2, 1988	0.002	0.000	1.403	0.009	0.756	0.005	46305	0	0			
K3, 1988	0.003	0.000	1.434	0.011	0.791	0.005	33358	0	0			
14305, 393												
K1	0.003	0.000	1.485	0.028	0.833	0.010	4676	1	0	1.6	0.9	0.0
K2	0.002	0.000	1.543	0.033	0.861	0.022	3560	0	0	1.3	0.0	0.0
K3	0.004	0.000	1.472	0.029	0.850	0.012	4234	5	1	1.5	4.7	0.9
K4	0.005	0.001	1.481	0.031	0.870	0.015	3692	4	0	1.3	4.3	0.0
PLAG	0.018	0.007	0.852	0.128	2.210	0.290	158	0	0	0.0	0.0	0.0
73215, 352												
K1	0.003	0.000	1.407	0.016	0.815	0.011	12389	1708	2824	4.0	551.5	911.8
K2	0.002	0.000	1.500	0.022	0.865	0.014	7418	19	52	2.5	10.2	28.0
K3	0.003	0.000	1.478	0.023	0.846	0.016	7013	157	190	2.4	89.5	108.4
PL1	0.002	0.000	1.501	0.021	0.856	0.015	8065	8	55	2.7	4.0	27.3
PL2	0.002	0.000	1.481	0.021	0.882	0.012	8404	10	111	2.9	4.8	52.8
14163, A												
1	0.013	0.006	1.453	0.070	1.117	0.081	672	1	0	0.5	6.0	0.0
2	0.006	0.002	1.320	0.071	1.057	0.066	573	0	2	0.4	0.0	14.0
3	0.011	0.003	1.283	0.077	0.998	0.068	446	0	0	0.3	0.0	0.0
4	0.007	0.001	1.372	0.055	0.922	0.069	1077	0	0	0.7	0.0	0.0

Table 1. (Continued)

Sample	204/206	±	207/206	±	208/206	±	206 cts	UO cts	ThO cts	Pb ppm	U ppb	Th ppb
14303, 330												
2	0.005	0.003	1.236	0.124	1.021	0.116	164	0	0	0.1	0.0	0.0
3	0.003	0.000	1.348	0.037	0.856	0.017	6531	33	335	2.6	20.2	205.2
4	0.005	0.001	1.528	0.040	0.903	0.029	4180	0	0	1.8	0.0	0.0
5	0.003	0.001	1.484	0.035	0.872	0.019	3168	0	7	1.3	0.0	8.8
15405, 57												
1	0.004	0.002	1.403	0.097	1.016	0.090	596	4	5	0.2	26.8	33.6
2	0.002	0.002	1.346	0.096	1.038	0.054	484	0	0	0.2	0.0	0.0
3	0.002	0.001	0.961	0.040	1.057	0.027	3959	6	43	1.3	6.1	43.4
4	0.003	0.001	1.124	0.030	0.983	0.021	2686	2	1	0.9	3.0	1.5
5	0.002	0.000	0.902	0.028	0.979	0.010	5157	0	4	1.7	0.0	3.1
15405, 145												
1	0.004	0.001	1.290	0.028	0.984	0.033	4154	0	3	1.4	0.0	2.9
2	0.002	0.000	1.462	0.031	0.984	0.025	4035	1	0	1.4	1.0	0.0
3	0.001	0.000	1.225	0.025	0.942	0.014	4321	0	0	1.4	0.0	0.0
4	0.003	0.001	1.111	0.021	1.016	0.018	5226	0	2	1.7	0.0	1.5
15405, 166												
1	0.011	0.001	0.983	0.024	1.085	0.028	3674	0	0	1.2	0.0	0.0
2	0.004	0.001	0.751	0.013	0.982	0.019	7647	66	1498	2.2	34.5	783.6
3	0.006	0.001	1.009	0.033	1.000	0.035	3754	0	23	1.2	0.0	24.5
4	0.012	0.004	0.950	0.076	1.121	0.084	783	41	56	0.3	209.5	286.1
5	0.008	0.005	1.059	0.057	1.170	0.074	662	1	3	0.3	6.0	18.1
6	0.002	0.004	1.181	0.088	0.980	0.039	497	9	49	0.2	72.4	394.4
8	0.004	0.002	1.038	0.054	1.007	0.059	710	12	25	0.3	67.6	140.8
9	0.005	0.002	1.318	0.068	1.148	0.068	634	0	9	0.3	0.0	56.8
10	0.003	0.002	1.397	0.102	0.989	0.062	513	0	0	0.2	0.0	0.0

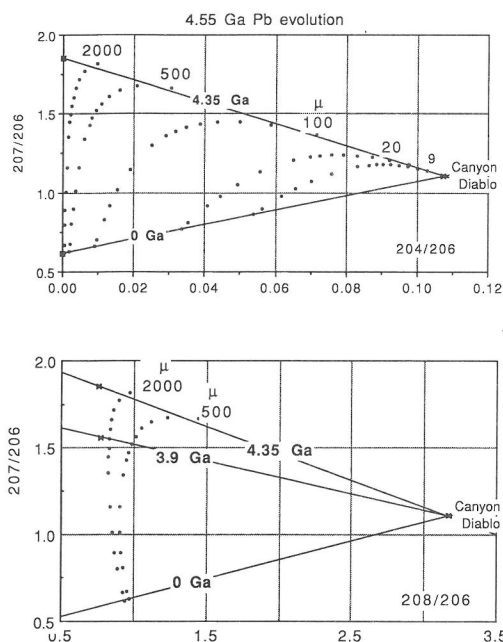


FIG. 2. Evolution of Pb composition with time in reservoirs of different μ ($^{238}\text{U}/^{204}\text{Pb}$), starting at 4.55 Ga with a Pb composition the same as that in Canyon Diablo. The straight lines are reference isochrons and the dotted curves represent different μ values ranging from 9 to 2000 (see text).

T_1 , μ_1 , and μ_0 are unknowns, but μ_0 might represent the original Moon and μ_1 the (local) lunar crust produced by differentiation at T_1 from which the granite will be formed later at T_2 . Equation (6) combined with the generalised Eqn. (4) may permit an exact solution for μ_1 and μ_0 at a nominated T_1 . Not all values of T_1 between T_0 and T_2 produce solutions, and sometimes no solutions are possible, which probably means that the feldspar has not preserved the initial isotopic ratios.

The y -intercept of the secondary isochron for the T_0 to T_1 stage is given by Eq. (1), which as T_1 approaches T_0 has the limiting value

$$^{207}\text{Pb}_*/^{206}\text{Pb}_* = \lambda_5 e^{(\lambda_5 - \lambda_8)T_0} / R\lambda_8 \quad (7)$$

which becomes 2.008 at 4.55 Ga. Two-stage solutions are possible if the measured feldspar $^{207}\text{Pb}/^{206}\text{Pb}$, $^{204}\text{Pb}/^{206}\text{Pb}$ point lies *below* the isochron corresponding to the above limit (joining 2.008 at zero $^{204}\text{Pb}/^{206}\text{Pb}$ with the Canyon Diablo Pb point in Fig. 2). Similarly, as T_1 approaches T_2 , Eqn. (7) gives the minimum value for $^{207}\text{Pb}_*/^{206}\text{Pb}_*$ (corresponding to the instantaneous production of radiogenic Pb at T_2) in a second-stage isochron. The measured feldspar point must lie *above* the line

joining this minimum to Canyon Diablo to obtain a possible two-stage solution.

RESULTS AND INTERPRETATION

Granite clasts younger than 4.0 Ga

The samples can be subdivided into groups: those whose ages are ≥ 4.3 Ga, which would certainly have experienced the late basin-forming major impacts, and those ≤ 4.0 Ga, some of which may have escaped.

Sawdust fragments, breccia 14163. The highest Pb content, 30 ppm, was found in Ba-rich feldspar in the granite clast B from breccia 14163, which shows well-preserved magmatic texture and mineralogy. There was detectable U and Th in only one of four areas analysed (B2.2, Table 1). Although the relative sensitivity factor for Pb^+ and UO^+ in feldspar is not known, the UO^+ counts are so low in comparison to Pb^+ that a significant contribution of *in situ* radiogenic Pb to the B2.2 analysis seems unlikely, nor is there any visible reduction in its isotopic ratios relative to the U-free areas. The Pb isotopic compositions of the four B2 areas are nearly equal within counting statistics and very radiogenic: high $^{207}\text{Pb}/^{206}\text{Pb}$ averaging 1.50 ± 0.02 (2σ) with low $^{204}\text{Pb}/^{206}\text{Pb}$ at 0.0029 ± 0.0002 (Fig. 3). Because of the high Pb concentration, its constant isotope ratios, and the excellent crystal preservation, we interpret the Pb as original magmatic Pb, and because of its highly radiogenic nature, as signifying magma generation from a long-lived source having very high μ (*ca.* 1500). The crystallization age of this particular granite is not known, but its single-stage model Pb age is 3.81 Ga. The source Th/U can be estimated from the measured $^{208}\text{Pb}/^{206}\text{Pb}$ of the feldspar and the inferred source μ , it is 4.15, consistent with direct measurements on other lunar rocks.

Two of the three areas analysed in the B1 clast have significantly lower $^{204}\text{Pb}/^{206}\text{Pb}$ and $^{208}\text{Pb}/^{206}\text{Pb}$ than B2, despite the much smaller Pb concentrations of these feldspars (Fig. 3). This is in the opposite direction to the greater blank effect expected in these samples; the differences would be enhanced if a blank correction were applied. The third area of B1 has isotope ratios much higher than B2, consistent with an added terrestrial contamination of *ca.* 2.5×10^{-16} g relative to the others, which is well within the range of possible blank variation. It follows that the initial Pb ratios for granite B1 were even more radiogenic than B2, so that the two cannot have crystallised from the same magma. All four analyses of the A1 granite clast are consistent with admixture of B2 type initial Pb with small

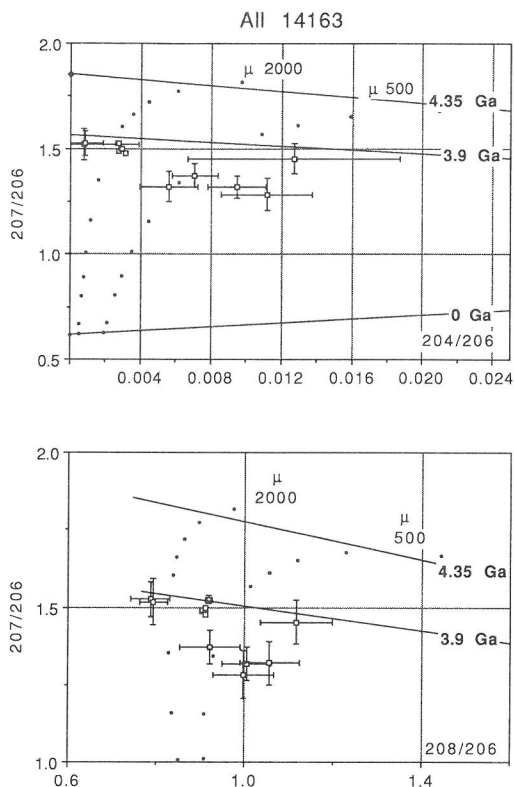


FIG. 3. Pb compositions measured on feldspar from sawdust fragments from breccia 14163 plotted on Pb evolution diagrams. Reference single stage isochrons for 4.35, 3.9 and zero Ga are shown, as are evolution curves for μ values of 500 and 2000.

amounts of contamination, but their Pb contents are too small for detailed interpretation.

14321, 1027. The petrology and chemistry of this clast has been described by WARREN *et al.* (1983). It is brecciated and contains 30% shock-melted glass, but undamaged areas showing igneous texture remain. Its crystallisation age has been determined at 3.96 ± 0.02 Ga by ion probe using cogenetic zircons (MEYER *et al.*, 1991).

Previous ion probe data on K-feldspars from this granite are well-fitted to a $^{204}\text{Pb}/^{206}\text{Pb}$ vs. $^{208}\text{Pb}/^{206}\text{Pb}$ mixing line between terrestrial Pb contamination and the mean of new data collected as described above (Fig. 4). We attribute that to surface-related Pb that remained in the former, and only the new data will be described here.

Five of the six new $^{208}\text{Pb}/^{206}\text{Pb}$ analyses agree to within error; the sixth is high in the direction of contamination and comes from an area having one-third of the Pb contents of the rest (Table 1). However, the ranges in $^{204}\text{Pb}/^{206}\text{Pb}$ and $^{207}\text{Pb}/^{206}\text{Pb}$ be-

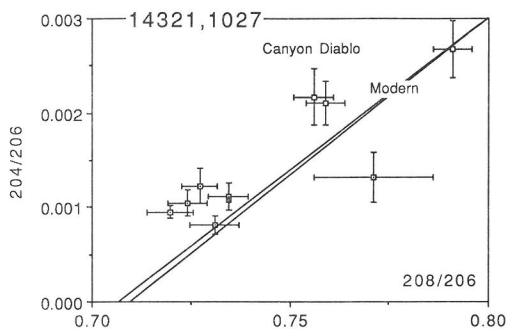


FIG. 4. Analyses of K-feldspar from granite clast 14321, 1027, plotted to show compositional variation consistent with mixing between a radiogenic end-member and common contaminant Pb.

tween different areas slightly exceed counting errors. Because of the high Pb contents and pristine nature of these samples, we consider that the mean values 1.429 ± 0.018 and 0.00102 ± 0.00014 for $^{207}\text{Pb}/^{206}\text{Pb}$, $^{204}\text{Pb}/^{206}\text{Pb}$ are at least dominated by the initial magmatic Pb, but the internal variation within

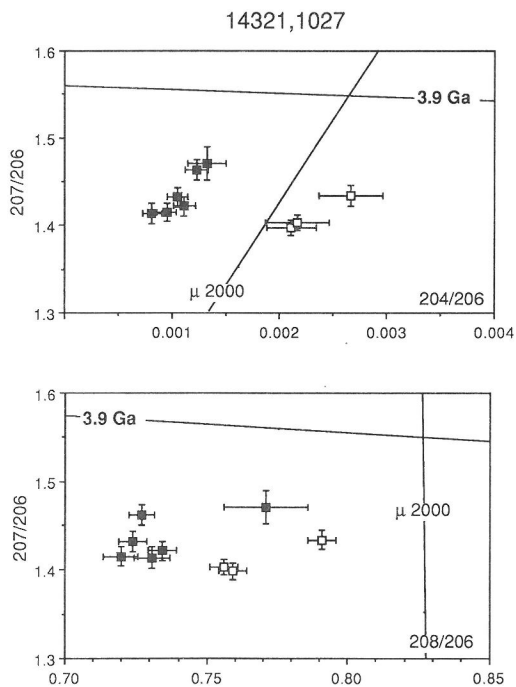


FIG. 5. Analyses of K-feldspars from granite clast 14321, 1027, showing the extremely uniform and highly radiogenic nature of their magmatic initial Pb. The single-stage isochron for 3.9 Ga and evolution curve for a μ value of 2000 are shown for reference. Open symbols indicate early analyses contaminated by surface Pb. Note greatly expanded scale on abscissa.

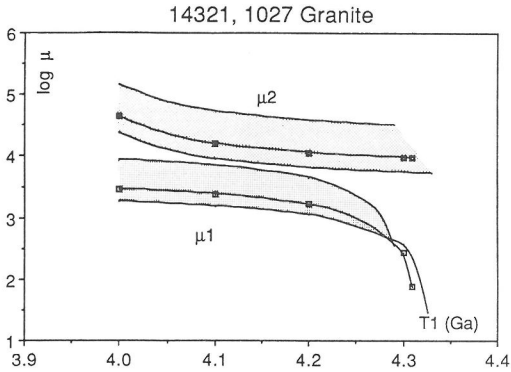


FIG. 6. Plot of $\log \mu$ vs. time (Ga), showing solutions to two-stage modelling of the inferred initial Pb composition measured on K-feldspar from granite clast 14321, 1027. Possible values of first and second stage μ (μ_1 and μ_2 , respectively) for different possible values of T_1 (the time of extreme Pb loss from the granite's source) are shown as shaded bands.

the feldspar might be real and if so, it signifies later alteration in the ratios (Fig. 5). All the ratios differ significantly from those of the 14163 granite fragments, and they lie within the allowed space between the single-stage 3.96 Ga isochron to 1.5937 for $^{207}\text{Pb}_*/^{206}\text{Pb}_*$ and the minimum μ_1 isochron to 1.171, thus two-stage solutions are possible.

The results of two-stage modelling based on $^{207}\text{Pb}/^{206}\text{Pb}$ and $^{204}\text{Pb}/^{206}\text{Pb}$ are shown in Fig. 6. The maximum value allowable for T_1 cuts off sharply at 4.32 Ga. During the preceding T_1 to T_0 period, μ_0 must be low but a definite value cannot be given because multiple solutions are allowed. For all T_1 , values for μ_2 are very high, at least 5000.

Does the sharp cut-off at 4.32 Ga correspond to a real lunar event? Pb isotopes will not answer that question conclusively, but only the lower values for μ_1 , which require the older choice for T_1 , are realistic in view of direct measurements on lunar highland rocks (TERA *et al.*, 1974). In addition, there is direct evidence for lunar magmatism between 4.32 Ga and 4.37 Ga in the form of widespread zircon crystallisation (MEYER *et al.*, 1991), besides still older isotopic ages by other methods (CARLSON and LUGMAIR, 1988). In terms of source history for the 14321, 1027 granite, we visualize a low μ part of the lunar crust or mantle as old as 4.55 Ga that was transformed at 4.31 Ga to a high μ source by extreme loss of Pb (crystal fractionation and/or degassing). The high μ source then accumulated radiogenic Pb from 4.31 Ga until 3.96 Ga, when it melted to form the granite as an extreme crystal fractionate and incorporated most of the source U and Pb.

If the feldspar Pb ratios have been appreciably altered, the above modelling is invalid. Suppose that the apparent $^{207}\text{Pb}/^{206}\text{Pb}$ was too low due to thermally induced isotope exchange with young radiogenic Pb. Choose a higher value, 1.56, which permits effectively a single-stage evolution from 4.55 Ga, for which μ will be *ca.* 5600 for any choice of T_1 . Even with this arbitrary adjustment of the data, a high μ is indicated for the granite source.

73215, 352. The petrology, genesis and history of this small clast of glass and relict crystalline rock was discussed by JAMES (1977). The age of either igneous crystallisation or glass formation is 3.91 ± 0.04 Ga by Ar-Ar and an internal Rb-Sr isochron; its maximum age is 4.0 Ga (COMPSTON *et al.*, 1977; JESSBERGER *et al.*, 1977).

Two areas of K-feldspar contained some U and Th (Table 1) and their $^{207}\text{Pb}/^{206}\text{Pb}$ and $^{208}\text{Pb}/^{206}\text{Pb}$ have been lowered by *in situ* radiogenic Pb (Fig. 7). The remaining three areas agree in all ratios to within counting statistics, giving means of 1.494 ± 0.023 for $^{207}\text{Pb}/^{206}\text{Pb}$ and 0.0020 ± 0.0003 for $^{204}\text{Pb}/^{206}\text{Pb}$. The conditions for two-stage modelling are met, and results show a cut-off of possible values

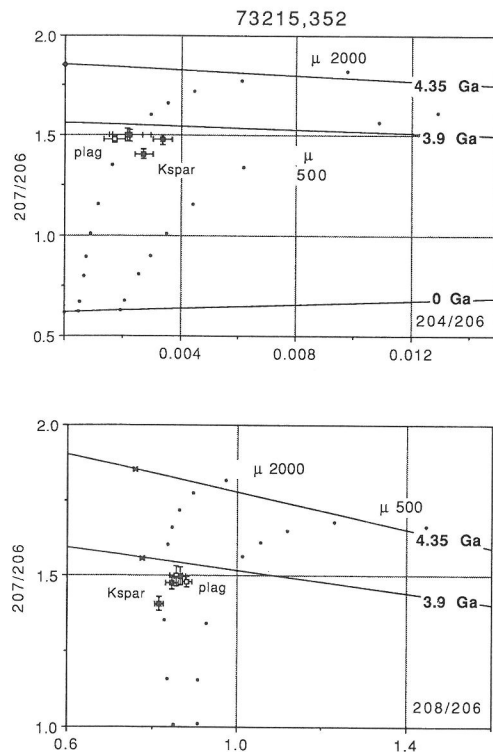


FIG. 7. Plot showing the similar Pb isotopic analyses of K-feldspar and plagioclase from felsite clast 73215, 352. Reference lines and curves as in Fig. 3.

for T_1 at 4.46 Ga, with low but non-specific μ_0 and high μ_1 at ≤ 3000 . As T_1 is reduced, μ_0 increases rapidly and μ_1 slowly. Thus, evolution of μ for the 73215, 352 felsite source follows that described for the 14321, 1027 granite: a long-lived penultimate source having very high μ preceded by one having permissibly low μ , with the difference that the high μ source for the 73215 felsite may have formed 0.1 Ga earlier. However, the timing for maximum T_1 depends sensitively upon the age T_2 of the felsite; if the latter is taken as 4.0 Ga, the maximum T_1 is reduced to 4.38 Ga. It is therefore important to obtain a zircon U-Pb age for the felsite.

72275, 20. STOESER *et al.* (1974) describe the chemistry and petrography of alkali-rich microgranite clasts from this and other Apollo 17 Boulder 1 samples. Their age has been determined as 4.03 ± 0.03 Ga, on the basis of Rb-Sr analyses of breccia matrix rich in the microgranite (COMPSTON *et al.*, 1975).

The Pb contents of the feldspars are fairly uniform regardless of type and lower than K-feldspars described here so far, and free of detectable U, Th except for a small ThO^+ count in area P1 (Table 1). As in the other granites, the isotope ratios are highly radiogenic, so a high μ source is again indicated.

In detail, the relative ratios do not detect any variable surface contamination. The mean plagioclase and K-feldspar ratios per area occur as separate groups in $^{208}\text{Pb}/^{206}\text{Pb}$ vs. $^{204}\text{Pb}/^{206}\text{Pb}$ coordinates, mainly because of the lower $^{204}\text{Pb}/^{206}\text{Pb}$ of the plagioclases; but the two do not lie on a mixing-line with terrestrial (or Canyon Diablo) Pb. They are uniform within error in $^{207}\text{Pb}/^{206}\text{Pb}$ except for one area which is low, and detectably spread in $^{204}\text{Pb}/^{206}\text{Pb}$ (Fig. 8). This might indicate early exchange with (external) radiogenic Pb having $^{207}\text{Pb}/^{206}\text{Pb}$ of *ca.* 1.2, but it cannot be due to Pb contamination. In view of the occurrence of the granite clasts as tiny fragments immersed in an impact melt, some Pb isotope exchange might be expected.

Some areas show apparent positive correlations between $^{207}\text{Pb}/^{206}\text{Pb}$ and $^{208}\text{Pb}/^{206}\text{Pb}$ within the serially measured seven ratios per analysis. This is maintained by the combined plot of all individual ratios, including $^{204}\text{Pb}/^{206}\text{Pb}$, supporting the possibility of early metamorphic Pb exchange but making it difficult to identify the magmatic Pb with confidence. On the grounds that the K-feldspar Pb appears to be the least or even not exchanged, we have chosen its mean ratios, 1.458 for $^{204}\text{Pb}/^{206}\text{Pb}$ and 0.0036 for $^{204}\text{Pb}/^{206}\text{Pb}$, as the best estimate for initial Pb.

Two-stage modelling again shows a sharp cut-off

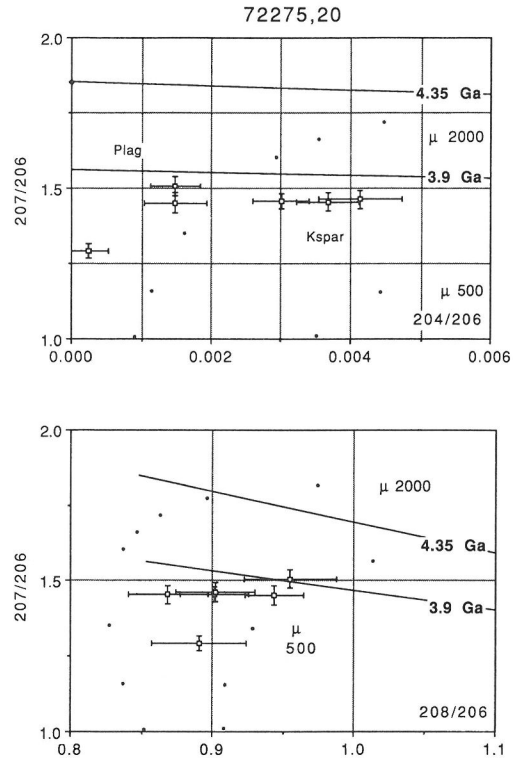


FIG. 8. Analyses of K-feldspar and plagioclase from microgranite clast 72275, 20. Reference single-stage isochrons for 4.35 and 3.9 Ga are shown, as are growth curves for μ values of 500 and 2000. Note the change in scale of the abscissa compared to the previous graphs.

for possible values of T_1 at 4.31 Ga. An unspecified but low μ_0 is allowed between 4.55 and 4.31 Ga, followed by μ_1 of at least 3200 until magma generation at 4.0 Ga.

12033, 567. This granite is mainly a fine-grained intergrowth of K-feldspar and silica, partly veined by brown glass and found as a small glass-coated fragment in the lunar soil (WARREN *et al.*, 1987). Its magmatic age has been measured by zircon U-Pb as 3.90 ± 0.01 Ga (MEYER *et al.*, 1991), with evidence in the zircons for variable and late decrease in $^{206}\text{Pb}/^{238}\text{U}$. The Ar-Ar age of the glass was measured by EBERHARDT *et al.* (1973) at 800 ± 40 Ma, which we take to be the Pb loss event.

The K-feldspars contain more than a factor of five greater Pb concentrations than the plagioclases (Table 1), and because the measured ratios show variable Pb contamination in the latter (Fig. 9), we do not consider the plagioclase data further. Early K-feldspar analyses made at lower sensitivity show very low $^{204}\text{Pb}/^{206}\text{Pb}$ which are technically suspect, but the other ratios are consistent with

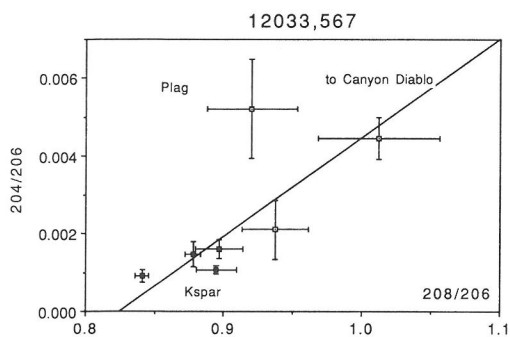


FIG. 9. Analyses of K-feldspar and plagioclase from granite clast 12033, 567, showing the effects of Pb contamination on the composition of the Pb in the plagioclase.

the new results. The first-order result is again the highly radiogenic Pb found, demanding a long-lived high μ source. In detail, there is a distinct range in the collective $^{207}\text{Pb}/^{206}\text{Pb}$, which has a weak negative correlation with $^{208}\text{Pb}/^{206}\text{Pb}$ for which there is no known *single* mixing end-member (Fig. 10). This is not due to *in situ* radiogenic Pb as two of the analysed areas are devoid of U, Th and there is no correlation with the amounts shown in the others. It probably signifies a combination of Pb contamination, possibly meteoritic, and isotope exchange with radiogenic Pb displaced from U-rich minerals, as such Pb is known to have been lost from the associated zircons. This makes it difficult to estimate the original magmatic Pb composition, but we have taken the highest measured $^{207}\text{Pb}/^{206}\text{Pb}$, 1.355 ± 0.018 , as a minimum value, and combined it with the mean of the new $^{204}\text{Pb}/^{206}\text{Pb}$ analyses, 0.0013 ± 0.0003 , for two-stage modelling.

With these parameters, the limiting value allowed for the maximum T_1 is lower than in previous granites; it is ≤ 4.25 Ga, at which a low μ from 4.55 Ga must be increased to 7600. A greater value for the initial $^{207}\text{Pb}/^{206}\text{Pb}$ would increase the maximum T_1 , and greater initial $^{204}\text{Pb}/^{206}\text{Pb}$ would permit lower μ_1 .

The mean apparent Th/U as calculated from the K-feldspar analyses is 4.2.

14305, 393. This is a clast of VHK basalt (Very High K) from breccia 14305, rather than lunar granite. It was selected for analysis for its abundant K-feldspar, which contains enough Pb for reliable ratio measurements (1.5 ppm) although the plagioclase does not, having the lowest (apparent) Pb contents that we have encountered so far, 0.025 ppm. $^{207}\text{Pb}/^{206}\text{Pb}$ and $^{208}\text{Pb}/^{206}\text{Pb}$ in four areas of K-feldspar agree to within counting statistics at 1.496 ± 0.032 and 0.845 ± 0.016 , respectively, and

$^{204}\text{Pb}/^{206}\text{Pb}$ nearly to within error at 0.0039 ± 0.0007 (Fig. 11). The single-stage model age for this Pb is 3.81 ± 0.07 Ga, within error of the crystallisation age as determined by a Rb-Sr internal isochron at 3.75 Ga (SHIH *et al.*, 1986).

The radiogenic initial Pb requires high μ at 1130 for a single-stage source, but the data also permit a complete range of two-stage source models between ≥ 3.81 Ga for T_1 up to ≤ 4.55 Ga. These differ from other samples analysed so far first, in having no discontinuity in T_1 that might signify a major Pb loss event in the lunar source, and secondly, in requiring that the first stage μ must be the greater, for example μ_0 1260 and μ_1 940 for the latter beginning at 4.3 Ga. Regardless of the details, the K-feldspar Pb was produced in a high- μ long-lived source. If the Pb were truly indigenous, then the VHK basalt source must have high μ , in contrast to mare basalts which have comparatively low μ . SHIH *et al.* (1986) propose that VHK basalt magmas

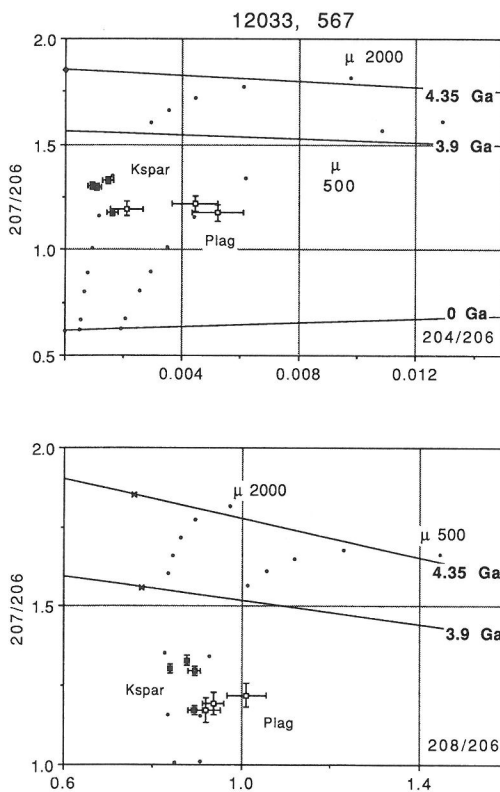


FIG. 10. Analyses of K-feldspar and plagioclase from granite clast 12033, 567. The K-feldspar Pb isotope compositions are less radiogenic than in other samples, probably because of exchange with younger radiogenic Pb displaced from U-rich minerals. Reference lines and curves as for Fig. 3.

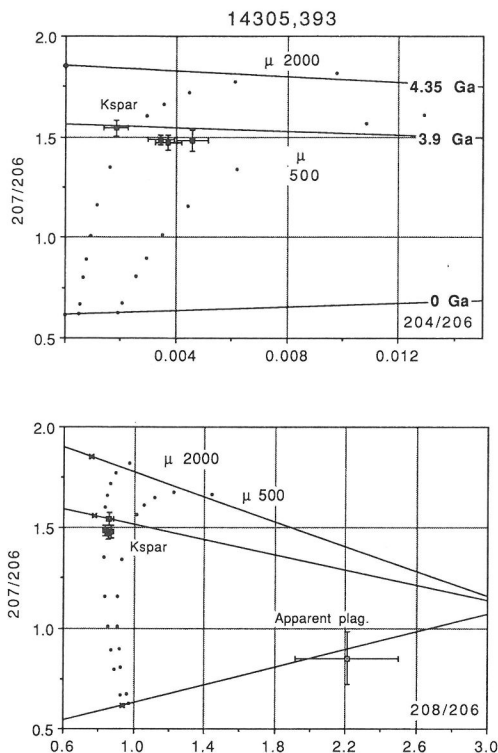


FIG. 11. Analyses of K-feldspar from clast 14305, 393, a very high K basalt, showing the extremely radiogenic initial Pb in the rock, much different from that of the apparent plagioclase (see text). Reference lines and curves as in Fig. 3. Note the change in scale of the abscissa compared to previous diagrams.

have been hybridised by assimilation of lunar granite, in which case their Pb isotope signatures would be dominated by the latter and the basalt source masked.

Granite clasts older than 4.0 Ga

14303, 1027. WARREN *et al.* (1983) have described and analysed this shock-melted granite clast. Some areas retain a coarse-grained graphic texture, and a few grains of diaplectic K-feldspar remain unmelted. The original age of crystallisation is reliably known as ≥ 4.32 Ga (MEYER *et al.*, 1991), through ion probe U-Pb dating of euhedral, presumably comagmatic zircon grains within the clast. Multiple analyses have been made of K-feldspar and, mainly, plagioclase in three polished thin sections of the clast (Fig. 1). Altered zones within the feldspars contain U and Th, especially in the PTS 14303, 205, but other areas are devoid of those elements and free of fractures. The Pb concentrations vary considerably, but most were on the order of 1

ppm. Despite the comparatively low Pb level, we are not aware of any effects due to surface contamination in the U- and Th-free areas except for one extremely low-Pb area (33.2, Table 1).

All Pb isotope data from the 14303 feldspars share two features: high $^{207}\text{Pb}/^{206}\text{Pb}$ that averages 1.56 and a distinct internal trend when displayed in $^{207}\text{Pb}/^{206}\text{Pb}$ vs. $^{208}\text{Pb}/^{206}\text{Pb}$ coordinates (Fig. 12). This trend is wrong for admixture with meteoritic or terrestrial contamination, but it is consistent with contamination by external Pb characterised by $^{207}\text{Pb}/^{206}\text{Pb}$ at ca. 1.45 and $^{208}\text{Pb}/^{206}\text{Pb}$ ca. 0.85 (Fig. 12), which could form in U-rich mineral phases outside the analysed areas. Presumably the mechanism for contamination was thermally induced Pb isotope exchange which accompanied the high temperatures to which the clast was plainly exposed. On this interpretation, the true initial $^{207}\text{Pb}/^{206}\text{Pb}$ for the granite will be at the higher end of the measured range, say 1.65, or beyond. Its upper limit will be 1.78, corresponding to single-stage U/Pb evolution from 4.55 to 4.32 Ga in a source having high μ (ca. 1500). (We can think of no process that would disperse the magmatic ratios towards higher $^{207}\text{Pb}/^{206}\text{Pb}$.)

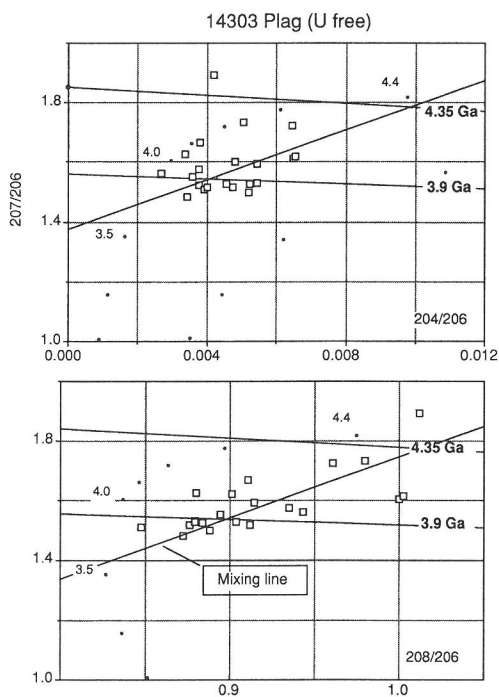


FIG. 12. Analyses of U-free plagioclase from granite clast 14303, 1027, showing a dispersion in composition consistent with mixing between initial Pb and radiogenic Pb. Scale of coordinates, reference lines, and curves as in Fig. 8.

It has not been possible to make a convincing independent estimate of the initial Pb ratios owing to the above internal trend. Suppose that the true ratios correspond to the highest U-free $^{207}\text{Pb}/^{206}\text{Pb}$ that can agree with each other to within error. The weighted mean for this group of 12 values is 1.62 ± 0.02 (σ), and the corresponding $^{204}\text{Pb}/^{206}\text{Pb}$ from the (poorly controlled) two-error regression of the observed $^{204}\text{Pb}/^{206}\text{Pb}$ vs. $^{207}\text{Pb}/^{206}\text{Pb}$ is 0.0043. There are no possible two-stage paths from Canyon Diablo Pb to this point at the known age of the granite. A better estimate for the $^{204}\text{Pb}/^{206}\text{Pb}$ can be obtained via the assumed radiogenic Pb contaminant and the centroid of the $^{204}\text{Pb}/^{206}\text{Pb}$, $^{207}\text{Pb}/^{206}\text{Pb}$ regression, which gives 0.0060. However, there are no two-stage solutions for this also, which means that some higher point along the $^{207}\text{Pb}/^{206}\text{Pb}$, $^{204}\text{Pb}/^{206}\text{Pb}$ trend must be assumed. Various two-stage evolution models are possible above 1.65 for $^{207}\text{Pb}/^{206}\text{Pb}$ but results are sensitive to the numerical details. Nevertheless, it is clear that the 14303 granite source must have had high μ for most of the time between 4.55 and 4.32 Ga; it would be 1500 for a single-stage history (implying Pb depletion from the start of lunar existence) or higher during the second of any two-stage evolution.

15405. As already reported (COMPSTON *et al.*, 1989), plagioclase from the quartz monzodiorite clast in breccia 15405 (RYDER, 1976) records radiogenic initial Pb but low U and Th counts in the areas selected for analysis. This contrasts with thermal ionisation results for mineral grains from the same rock (TATSUMOTO and UNRUH, 1976), which gave much lower $^{207}\text{Pb}/^{206}\text{Pb}$ ratios (Fig. 13). The latter are evidently due to the high contents of U and Th present in the mineral separates and their resulting high contents of *in situ* radiogenic Pb. Very small U, Th-rich inclusions and/or fracture-fillings might occur in the hand-picked minerals, which can be avoided at the 30 μm sampling scale of ion-probe analysis. Combined, the two types of data indicate the mixing of leads of different origins: an initial Pb having $^{207}\text{Pb}/^{206}\text{Pb} \geq 1.33$; two *in situ* radiogenic leads corresponding to crystallization at 4.3 Ga and possible recrystallisation at *ca.* 1.2 Ga, which is the time of Pb loss seen in some areas of zircon (MEYER *et al.*, 1991) as well as the Pb-Pb age given by whitlockites (TATSUMOTO and UNRUH, 1976); and either a low- μ meteoritic Pb in the rock or in the quartz monzodiorite magma or else a surface terrestrial contamination which would displace data points to the right in Fig. 13. The apparent initial $^{207}\text{Pb}/^{206}\text{Pb}$ of 1.33 is too low to permit two-stage evolution from 4.55 Ga, and we infer that younger radiogenic Pb must have been added to the plagioclase during later metamorphism.

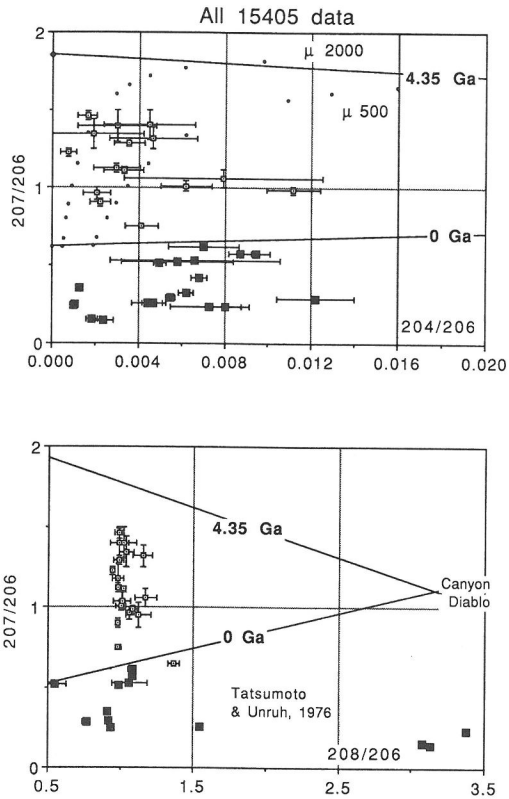


FIG. 13. Plots analogous to Fig. 2a and b, showing Pb analyses of minerals from the quartz monzodiorite clast in breccia 15405. Ion probe analyses of plagioclase (open symbols) show considerably higher $^{207}\text{Pb}/^{206}\text{Pb}$, and less dispersion in $^{204}\text{Pb}/^{206}\text{Pb}$ and $^{208}\text{Pb}/^{206}\text{Pb}$ than the thermal ionisation analyses of mineral separates by TATSUMOTO and UNRUH (1976).

SUMMARY AND CONCLUSIONS

1. In each of the eight clasts or fragments of lunar granite and in one VHK basalt examined, Pb is concentrated in well-preserved feldspars at up to *ca.* 30 ppm in certain Ba-rich feldspars. Also, nearly all of the inclusion-free areas of feldspar are devoid of U and Th at the sub-ppb level. This distribution is consistent with normal crystal-chemical controls in magmas. We therefore consider that this Pb is an original component of the granite magma, rather than introduced to the crystallised feldspars from an external source during later thermal events.
2. This Pb is very radiogenic, high in $^{207}\text{Pb}/^{206}\text{Pb}$ and very low in $^{204}\text{Pb}/^{206}\text{Pb}$. Such an isotopic composition labels the magma source as having had a very high μ , up to 2000, for several hundred Ma prior to magma generation.
3. The crystallisation ages of all samples except the three fragments from breccia 72275, 20 are

known by independent isotopic dating. This places a strong constraint on Pb isotope modelling of the magma sources.

4. Using (numerical) modelling based on the initial Pb isotopic composition of the individual granites, their exact ages, and the Canyon Diablo Pb starting-point, none of the magma sources for the ≤ 4.0 Ga granites had a single-stage μ evolution (except possibly the 72275, 20 granites). Two-stage evolution is mandatory, and at least one of the stages must have had very high μ . Nearly all sources are permitted a low- μ first stage, but the specific values cannot be determined.

5. The maximum time for the start of the second, high μ stage for several granites is *ca.* 4.3 Ga, which might signify a real lunar U-Pb fractionation event.

6. We have not succeeded in conclusively measuring the initial Pb isotope ratios in the two ≥ 4.3 Ga granites. Both are highly radiogenic, but their original ratios have been disturbed by addition of an external, younger radiogenic Pb. One, 14303, 205, has the highest lunar $^{207}\text{Pb}/^{206}\text{Pb}$ known at ≥ 1.65 , which is the mean of ratios at the high end of a mixing line in $^{207}\text{Pb}/^{206}\text{Pb}$, $^{208}\text{Pb}/^{206}\text{Pb}$ coordinates defined by the collective data from all analysed samples.

7. Even 1.65 is too low to allow a two-stage (or single-stage) μ evolution to 4.32 Ga. The true initial $^{207}\text{Pb}/^{206}\text{Pb}$ must be higher still, and we have no way of correcting for the external Pb. Feldspars from the other 4.3 Ga granite likewise fail to allow two-stage solutions.

8. For 14303, the approximate age of the external radiogenic Pb is 3.5–4.0 Ga, but much younger radiogenic Pb is indicated for 15405. The former might correspond with high temperatures associated with a basin-forming impact, but the latter does not and is evidently associated with a comparatively minor impact.

9. The ion probe SHRIMP is very suitable for Pb isotope studies on existing lunar thin-sections. The effective terrestrial blank is less than 1 femtogram and often < 0.1 fg. Useful results can be obtained at the level of 1 ppm (total) Pb at sensitivity 10 cps/ppm/primary nA. The Moon itself is favourable for the purpose owing to the very high μ in substantial volumes of its crust and mantle, which generates large changes in Pb isotopic composition with time.

REFERENCES

- CARLSON R. W. and LUGMAIR G. W. (1988) The age of ferroan anorthosite 60025 oldest crust on a young Moon? *Earth Planet. Sci. Lett.* **90**, 119–130.
- CLEMENT S. W. J. and COMPSTON W. (1989) SIMS at high sensitivity and high mass resolution. *Proc. 7th. Intl. Conf. Secondary Ion Mass Spectrometry*. J. Wiley & Sons.
- COMPSTON W., FOSTER J. J. and GRAY C. M. (1975) Rb-Sr ages of clasts from within Boulder 1 Station 2 Apollo 17. *The Moon* **14**, 445–462.
- COMPSTON W., FOSTER J. J. and GRAY C. M. (1977) Rb-Sr systematics in clasts and aphanites from consortium breccia 73215. *Proc. Lunar Sci. Conf. 8th*, 2525–2549.
- COMPSTON W., WILLIAMS I. S. and MEYER C. (1984) U-Pb geochronology of zircons from lunar breccia 73217 using a sensitive high mass-resolution ion microprobe. *Proc. Lunar Sci. Conf. 14th; J. Geophys. Res.* **89**, B525–B534.
- COMPSTON W., WILLIAMS I. S. and MEYER C. (1989) The Problem of Lunar initial Pb (abstr.). *Lunar Planet. Sci. Conf. 20th*, 179.
- EBERHARDT P., GEISS J., GROGLER N. and STETTER A. (1973) How old is the crater Copernicus? *The Moon* **8**, 104–114.
- JAMES O. B. (1977) Petrology of four clasts from consortium breccia 73215 (abstr.). *Lunar Planet. Sci. Conf. 8th*, 502–504.
- JASSBERGER E. K., KIRSTEN T. and STAUDACHER TH. (1977) One rock and many ages—Further K-Ar data on consortium breccia 73215. *Proc. Lunar Sci. Conf. 8th*, 2567–2580.
- MEYER C., COMPSTON W. and WILLIAMS I. S. (1985) Lunar zircon and the closure age of the lunar crust (abstr.). *Lunar Planet. Sci. Conf. 16th*, 557–558.
- MEYER C., WILLIAMS I. S. and COMPSTON W. (1991) Direct evidence for ancient lunar granite (in prep.).
- RYDER G. (1976) Lunar sample 15405 Remnant of a KREEP basalt-granite differentiated pluton. *Earth Planet. Sci. Lett.* **29**, 255–268.
- SHIH C.-Y., NYQUIST L. E., BOGARD D. D., BANSAL B. M., WIESMANN H., JOHNSON P., SHERVAIS J. W. and TAYLOR L. A. (1986) Geochronology and petrogenesis of Apollo 14 very high potassium mare basalts. *Proc. Lunar Sci. Conf. 16th*, D214–D228.
- SILVER L. T. (1970) Uranium-thorium-lead isotopes in some Tranquillity Base samples and their implications for lunar history. *Proc. Apollo 11 Lunar Sci. Conf.; Geochim. Cosmochim. Acta Suppl.* **1**, 533–1574.
- STOESER D. B., MARVIN U. B. and BOWER J. F. (1974) Petrology and petrogenesis of Boulder 1. In *Interdisciplinary Studies of Samples from Boulder 1 Station 2 Apollo 17*. (ed. J. A. WOOD) Vol 2; *LSI Contrib. 211D*, III1–III51. Smithsonian Astrophysical Observatory, Cambridge, MA.
- TATSUMOTO M. (1970) Age of the Moon: An isotopic study of U-Th-Pb systematics of Apollo 11 lunar samples—II. *Proc. Apollo 11 Lunar Sci. Conf.; Geochim. Cosmochim. Acta Suppl.* **1**, 1595–1612.
- TATSUMOTO M. and UNRUH D. M. (1976) KREEP basalt age grain by grain U-Th-Pb systematics study of the quartz monzodiorite clast 15405 88. *Proc. Lunar Sci. Conf. 7th*, 2107–2129.
- TATSUMOTO M., PREMO W. R., UNRUH D. M. (1987) Origin of lead from green glass of Apollo 15426 A search for primitive lunar lead. *Proc. Lunar Sci. Conf. 17th; J. Geophys. Res.* **92**, E361–E371.
- TERA F., PAPANASTASSIOU D. A. and WASSERBURG G. J. (1974) Isotopic evidence for a terminal lunar cataclysm. *Earth Planet. Sci. Lett.* **22**, 1–21.
- WARREN P. H., TAYLOR G. J., KEIL K., SHIRLEY D. N. and WASSON J. T. (1983) Petrology and chemistry of two “large” granite clasts from the Moon. *Earth Planet. Sci. Lett.* **64**, 175–185.
- WARREN P. H., JERDE E. A. and KALLEMEYN G. W. (1987) Pristine Moon rocks: A large felsite and a metal-rich ferroan anorthosite. *Proc. Lunar Sci. Conf. 17th; J. Geophys. Res.* **92**, E303–E313.